MULTI-TEMPORAL IMAGE ANALYSIS FOR MONITORING THE CHANGES IN FUZZY SHORELINES

Ratna Sari Dewi[1,2], Wietske Bijker[1] and Alfred Stein[1]

[1]Faculty of Geo-information Science and Earth Observation (ITC), University of Twente,
PO.Box 217, 7500 AE Enschede – The Netherlands;
Email: r.s.dewi@utwente.nl, w.bijker@utwente.nl, a.stein@utwente.nl

[2]Geospatial Information Agency (BIG),
Jl. Raya Jakarta-Bogor Km. 46, Cibinong, Bogor, 16911 – Indonesia

KEY WORDS: shoreline change; confusion index; coastal inundation; Indonesia.

ABSTRACT: The mapping of shorelines and monitoring of their changes is challenging due to the large variation in shoreline position related to seasonal and tidal patterns. This study focused on a flood-prone area in the north of Java. Shoreline mapping and monitoring are needed to support efforts to recover the eroded land and to reduce the rapid shoreline degradation. We show the possibility of using fuzzy-crisp objects to derive shoreline positions as the transition zone between the classes *water* and *non-water*. Fuzzy c-means classification (FCM) was used to estimate the membership of pixels to these classes. A shoreline is represented by a transition zone between the classes, and its spatial extent was estimated by using fuzzy-crisp objects. We analyse the differences between successive shorelines from multi-temporal images. A change category was defined if the membership difference between two years T_1 and T_2, represented by change magnitude values, differs from zero, whereas a no-change category corresponded to a magnitude equal to zero. This resulted into an overall change magnitude and the change directions of the shoreline. It allowed us to jointly identify the trend of the fluctuating shoreline and the uncertainty distribution. Fuzziness of the positions of the shoreline was assessed by using change confusion values. The overall accuracies of FCM resulted into a fuzzy error matrix (FERM) with values ranging from 0.84 to 0.90. Change areas were identified as well as the magnitude, direction and confusion values of the changes for the observed objects at the pixel level. The proposed method provided a way to analyse changes of shorelines as fuzzy objects and is well-suited to apply to coastal areas around the globe.

1. INTRODUCTION

The study of changing shoreline is essential to assist in the design of effective coastal protection (Jin *et al.* 2015), developing hazard maps (Snoussi *et al.* 2009), formulating policies regarding coastal development (O'Connor *et al.* 2010) and for coastal research and monitoring (Tamassoki *et al.* 2014). A shoreline is defined as the intersection of coastal land and water surface indicating the water edge movements of which the position is changing through time due to different water levels during high tide and low tide (Boak and Turner 2005; Davidson-Arnott 2010; Bird 1985). Shorelines have changed their dynamics at varying rates as a response to coastal processes such as sediment erosion, transportation and deposition along the shore. Shoreline changes can be estimated over various time scales and result into long-term, cyclic and local random variation. Long-term variation includes variation due to the land subsidence, relative sea level rise and sediment storage. Cyclic variation is related to the tide cycles or seasons, whereas waves, storms and floods cause random variation of a local character.

Previous studies have proposed several ways of generating shoreline positions. Shoreline survey and photogrammetry have been the primary technology for shoreline mapping, yet both methods are time consuming and expensive (Li *et al.* 2002). Therefore, image classification is widely used to detect shoreline positions. Most studies regarding shoreline detection have used hard classification such as thresholding, water indices, and manual digitizing (Ghosh *et al.* 2015; Senthilnatha *et al.* 2012; Marfai *et al.* 2008), and only a few applied soft classifications (Muslim *et al.* 2006; Dewi *et al.* 2016). Shoreline represents the physical interface between coastal land and water surface which varies continuously over time. Moreover, the boundary between coastal land and water is imprecise and there is a gradual transition between them. Due to the fuzziness of shoreline positions, using hard classification for shoreline mapping could produce errors on the classification results, since hard classification assigns a single label to a pixel based on its highest membership. To overcome this limitation, fuzzy classification is explored to detect shoreline positions. In our previous work, we proposed two approaches: 1) the first approach derived shorelines by applying a threshold equal to 0.5 to the membership and depicted shorelines as a single line; and 2) the second approach derived shorelines as a margin determined by the choice of thresholds on the membership function (Dewi *et al.* 2016). In this work, we proposed the third approach and shorelines are

represented as the transition zone between water and land. In this case, points at which membership (μ) larger than 0.99 are the interior of objects, whereas points with $0.01 < \mu < 0.99$ would belong to transition zones and points with $\mu < 0.01$ do not belong to objects.

The objective of this study is to develop a fuzzy method that is useful for monitoring the changes of a fuzzy shoreline. The method is based on fuzzy classification and change vector analysis (CVA) was used to estimate the changes of the successive shorelines. This CVA provides an overall change magnitude and change directions showing the trend of the fluctuating shoreline from 2013 to 2015. A series of Landsat images are used to detect shoreline positions while taking tides into account. For this study, the uncertainty of shoreline positions was estimated by means of confusion indices. The method is applied to an area in Java - Indonesia, where the changes of shoreline are associated with coastal inundation.

2. METHODOLOGY

2.1. Study Area

The study area is located in the northern part of Central Java, Indonesia (see Figure 2a) characterized by a low-land landscape extending 5 km from east to west with elevation less than 5 m above mean sea level (AMSL). Two types of flood regularly occur: (1) floods caused by a tidal flood occurring daily (Harwitasari and van Ast 2011); and (2) floods due to poor drainage systems during rainy seasons. The coastal inundation has increased recently in terms of both frequency and duration. Some factors such as extreme winds and waves contribute to this increase over the short term. Furthermore, over the long term, other causes such as land subsidence, mangrove conversion, beach reclamation and an extended seaport are the causes for the increase of coastal inundation (Marfai and King 2007).

2.2. Satellite Images and Data Pre-processing

Multi-temporal images from the Landsat OLI/TIRS (Operational Land Imager/Thermal Infrared Sensor) with 30 m spatial resolution were used to monitor the shoreline change between 2013 and 2015. Those images were acquired at the low tides (Table 1). The classification results were validated against three higher resolution images.

Table 1. Landsat OLI/TIRS images captured in the low tides supplemented by tide level and reference images

Acquisition Date	Astronomical Tide Level (m)	Reference Data	Acquisition Date	Astronomical Tide Level (m)	Reference Data
23 May 2013	-0.1	Pleiades	1 Oct 2014	-0.2	Spot 6
12 Sept 2013	-0.1	(27 Feb 2013)	18 Nov 2014	-0.3	(5 Oct 2014)
14 Oct 2013	-0.3		29 May 2015	+0.04	
1 Dec 2013	-0.3		18 Sept 2015	-0.1	Sentinel 2
10 May 2014	-0.01	Spot 6	20 Oct 2015	-0.3	(26 Dec 2015)
15 Sept 2014	-0.2	(5 Oct 2014)	21 Nov 2015	-0.3	

Pre-processing for Landsat and reference images comprises two steps: 1) histogram minimum adjustment (Hadjimitsis *et al.* 2010); and 2) geo-referencing implemented using >100 ground control points (GCP) collected from road intersections and other prominent features. The root mean square error (RMSE) values were less than 0.1 pixels. Reference images were rectified using the 2015 ortho-image. Geo-registration of Landsat was conducted using geometrically corrected reference images. For accuracy assessment purpose, pixel size of Spot 6 was resampled to 10 m, so that spatial resolutions of Pleiades, Spot 6, Sentinel 2 and Landsat were in the ratio 15:3:3:1. Further, to reduce the variance of Pleiades, a smoothing was performed using the average filter with 3x3 window size.

2.3. Deriving Fuzzy Shoreline and Its Uncertainty

To discriminate the land and water classes, we applied the FCM method developed by Bezdek *et al.* (1984) with the number of classes $c = 2$. The membership values (μ) calculated using FCM have values ranging from 0 to 1. Detailed descriptions regarding the FCM algorithm are available in Bezdek *et al.* (1984), whereas explanations regarding membership function, pixel labelling, and parameter estimation for FCM are explained in Dewi *et al.* (2016). After classification, for each land cover class, memberships were represented as a raster layer and the number of raster layers is equal to the number of classes: *water* and *non-water* memberships, each with fuzzy regions and boundaries. To determine their spatial extent, we combined objects from different layers into one layer based on the work conducted by Cheng (1999). We consider the boundaries between *water* and *non-water* are fuzzy and forming a transition zone that we call *shoreline*. The decision function d_{wk} assigned pixel k which has

membership value μ_{wk} to *water* class (*w*). If ($\mu_{wk} > 0.99$) then let ($d_{wk} = 1$) then it means the pixels belong to *water* class. If ($0.01 < \mu_{wk} < 0.99$) then let ($d_{wk} = \mu_{wk}$) then it classifies pixels as the transition zones, and if ($\mu_{wk} < 0.01$) then let ($d_{wk} = 0$) then it means the pixels not belong to *water* and define the pixels as the *non-water* class. The uncertainty of shoreline positions was estimated by a measure of confusion index *CI* estimated as one minus the difference between the first and the second highest membership values μ_{ik}^{1} and μ_{ik}^{2} respectively (Burrough *et al.* 1997).

To quantify the accuracy of the FCM classifier, we used a fuzzy error matrix developed by Pontius and Cheuk (2006). For accuracy assessment, soft reference images were generated by applying FCM classification to the Pleiades, Spot 6, and Sentinel 2. To calculate the agreement in FERM, a group of 225 pixels (15x15) of Pleiades, 9 pixels (3x3) of Spot 6 and 9 pixels (3x3) of Sentinel 2 were averaged to achieve the pixel dimension of Landsat. Using this reference data, membership of 200 pixels randomly selected from both classified and reference images were computed. An overall accuracy was computed for each error matrix.

2.4. Shoreline Change Detection and Change Uncertainty

The changes of shoreline were assessed by simultaneous analysis of multi-temporal images using pixel-wise change vector analysis (CVA) to distinguish the changes in terms of magnitude and direction (Lambin and Ehrlich 1997; Singh and Talwar 2015). For establishing the changes over time, shoreline membership images of the same year were stacked together and then compared with the stack of shoreline membership images of the next year with corresponding seasons. If membership values to water class (μ_{wk}) of two images in years T_1 and T_2 are given by $G = (g_1, g_2, g_3, g_4)^{T_1}$ and $H = (h_1, h_2, h_3, h_4)^{T_2}$ respectively, a change vector is defined as:

$$\Delta CV = H - G = \begin{pmatrix} h_1 - g_1 \\ h_2 - g_2 \\ h_3 - g_3 \\ h_4 - g_4 \end{pmatrix} \tag{1}$$

where ΔCV includes all the change information between two dates for a given pixel. The length of the change vector indicates the magnitude of change and its direction indicates the nature of the change showing the trend of water membership in every pixel (Lambin and Strahler 1994; Lunetta and Elvidge 1999). The change magnitude $\|\Delta CV\|$ is computed by determining the Euclidean distance between the two images:

$$\|\Delta CV\| = \sqrt{(h_1 - g_1)^2 + (h_2 - g_2)^2 + (h_3 - g_3)^2 + (h_4 - g_4)^2} \tag{2}$$

This change magnitude represents the total of membership differences between two years. A *change* category was defined when the membership difference between two years T_1 and T_2 is larger than zero, whereas a *no-change* category is related to a magnitude equal to zero. Change direction was determined by evaluating the membership difference between images in two successive years starting by calculating the number of change combinations (*CC*):

$$CC = cd^z \tag{3}$$

where *cd* refers to the types of change direction when we compare the stack of shoreline membership images from both years per corresponding seasons and *z* refers to the number of membership image pairs. The change vector (CV) showing membership difference between a pair of shoreline images in T_1 and T_2 from corresponding seasons needed to be estimated: a) If the membership difference between pair of images in years T_1 and T_2 is less than zero then $CV = -1$ showing a decrease of water membership in T_2; b) If the membership difference is larger than zero then $CV = +1$ showing an increase of water membership in T_2; c) If the membership difference is equal to zero then $CV = 0$ showing that the membership in T_1 and T_2 were the same. *Total change vector* (*TCV*) values were defined as:

$$TCV = CV1 + CV2 + CV3 + CV4 \tag{4}$$

CV1 refers to $h_1 - g_1$, *CV2* refers to $h_2 - g_2$, *CV3* refers to $h_3 - g_3$, and *CV4* refers to $h_4 - g_4$. *Total change vector* values vary from -4 up to +4. Finally, the change direction (*Chg.dir*) categories showing the degree of change direction to water membership were obtained by grouping the direction values: a) *TCV* from +1 up to +4 were grouped as *positive change*; b) *TCV* from -4 up to -1 were grouped as *negative change*; c) *TCV* equal to 0

having membership differences equal to 0 for all *CV1, CV2, CV3* and *CV4* were classified as *no-change*; d) Total values equal to 0 showing unclear change directions for *CV1, CV2, CV3* and *CV4* were classified as *no-direction*. Based upon these results, the change area of a specific category was defined as:

$$Ar(Chg) = Pix_k(Chg) \times Ar(k) \quad (5)$$

where $Pix_k(Chg)$ is number of pixels of a specific change category, $Ar(k)$ is area of pixel k equal to 30 x 30 (m^2). The change uncertainty of changed areas was estimated using confusion index *CI* as the indicator to estimate the change confusion. If confusion indices of two images in years T_1 and T_2 are given by $Q = (q_1, q_2, q_3, q_4)^{T_1}$ and $R = (r_1, r_2, r_3, r_4)^{T_2}$, respectively, the change confusion $\|\Delta CU\|$ is computed as:

$$\|\Delta CU\| = \sqrt{(q_1 - r_1)^2 + (q_2 - r_2)^2 + (q_3 - r_3)^2 + (q_4 - r_4)^2} \quad (6)$$

3. RESULTS

3.1. Fuzzy Shorelines and Uncertainty Estimation

The results of FCM classification are presented in Figure 1a-b with the values ranging from 0-1. Figure 1c presents the core of *water* and *non-water* with their transition zone representing shoreline positions. The accuracy values vary from 0.84 – 0.90. Figure 1d presents the confusion index indicating the classification uncertainty when deriving shorelines. Figure 1e shows shorelines with fuzziness. These ambiguous areas indicate transition zones as the position of shorelines. The extent of these shorelines is determined by natural condition of the coastal areas, for example, a wider shoreline is found in a muddy area or at a gradual coast, whereas a narrow shoreline is usually found along an elevated coast or at the shoreline with embankment.

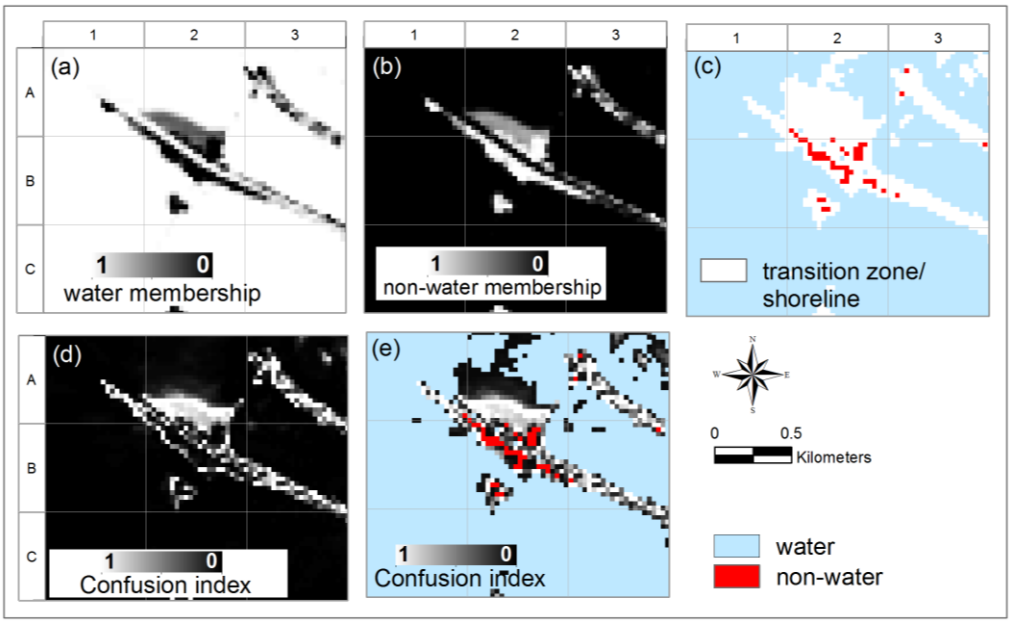

Figure 1. FCM results show the memberships of *water* (a) and *non-water* (b). The core of *water*, *non-water* and the *transition zone* indicating the shoreline positions (c); confusion index to quantify the classification uncertainty (d); and *shoreline* with fuzziness (e).

3.2. Shoreline Change Detection

The change magnitude and the c*hange* and *no-change* categories of shoreline are displayed in Figure 2b-c. Low change magnitude values presented as green pixels correspond to a small membership difference between water membership images in T_1 and T_2, whereas red pixels are associated with high magnitude corresponding to a large membership difference. The fuzziness of the change of shorelines is presented in Figure 2d-e. Low change confusion corresponds to the small confusion indices difference between images in T_1 and T_2 while high change confusion was associated with large confusion indices difference. The representation of change direction of shoreline showing the trend of water membership can be seen in Figure 3a-b. Figure 3c-d show the magnitude of the change identified for each change direction in 2013-2014 and 2014-2015, respectively.

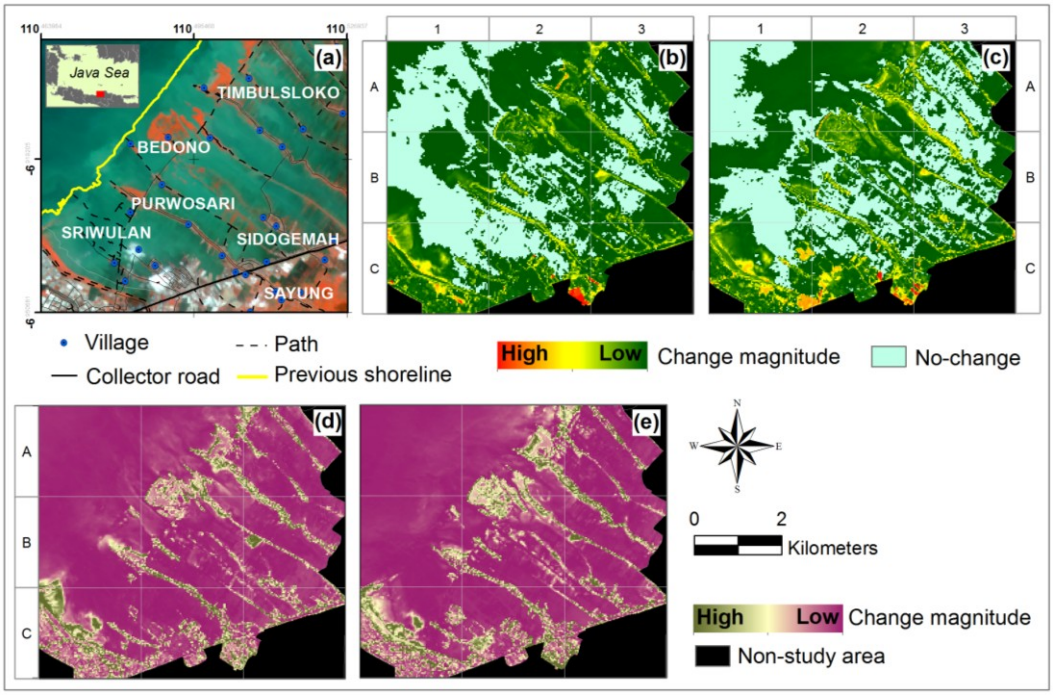

Figure 2. The study area with Landsat RGB 542 as the background. Red pixels refer to vegetation, green pixels refers to water and white and grey pixels refer to built-up areas (a);. The magnitude of shoreline change from 2013-2014 (b) and from 2014-2015 (c); The fuzziness of the shorelines is represented by change confusion values in 2013-2014 (d) and in 2014-2015 (e), respectively.

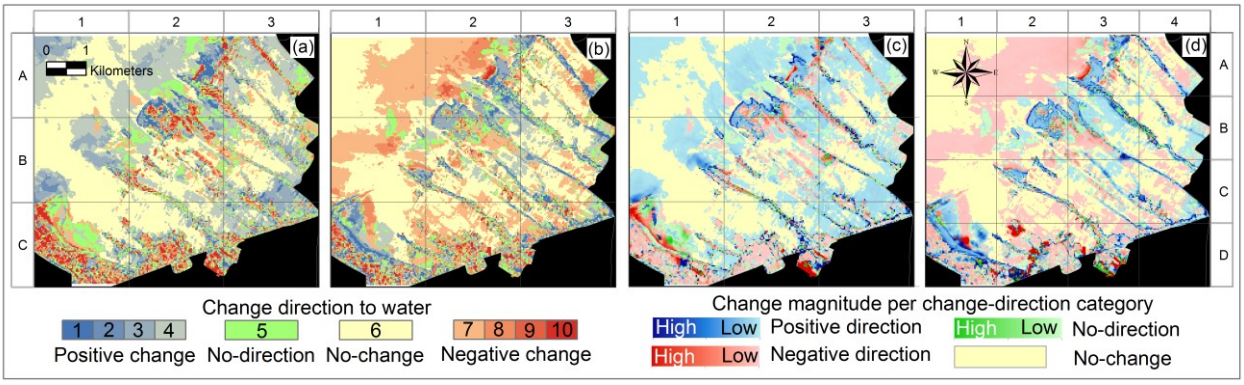

Figure 3. The representation of change direction of shorelines in 2013-2014 (a); and in 2014-2015 (b); and the magnitude of each change direction category for shoreline in 2013-2014 (c); and in 2014-2015 (d), respectively.

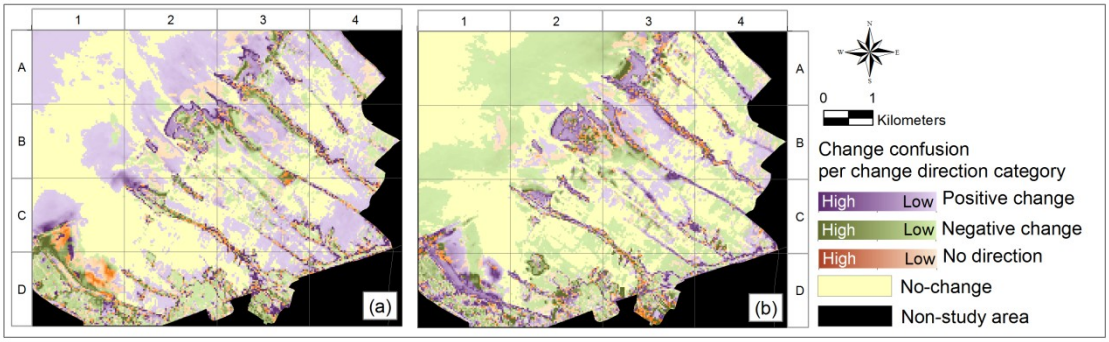

Figure 4. The change confusion indices for each change direction category in 2013-2014 (a); and in 2014-2015 (b), respectively. Shades of violet pixels represent change confusion values for the area with *positive changes* to water membership, and shades of moss green pixels show change confusion values for the area with *negative changes.* The change confusion values for the *no-direction* category are represented by shades of orange.

The intensity of the change confusion is identified for each change direction category in 2013-2014 and 2014-2015 as can be seen in Figure 4a and Figure 4b, respectively. Three change confusion values for each category including *positive*, *negative* and *no-direction* categories are presented by shades of violet, shades of moss green and shades of orange colours, respectively. Darker colours present higher change confusion values for each change category.

3.3. Multi-year Pattern of Water Membership Changes

For each pixel, the resulting change vector provides information regarding its change direction and magnitude which reveals that each combination represents specific type of change processes occuring in the field:

a) High change direction and high magnitude; indicates a continuous change of an area to a certain direction with a relatively large intensity. A consistency to *positive change* indicates a persistence of water influence as those pixels show an increase of water membership in multitemporal images. This probably corresponds to the land subsidence and coastal inundation (Figure 5a,c). On the other hand, a continuosly decreasing water membership in multitemporal images categorized as *negative change* direction may indicate a success in shoreline protection scheme (Figure 5b,d) such as the project *Building with Nature* which involves building permeable dams refered to as sediment traps (NWP 2016);

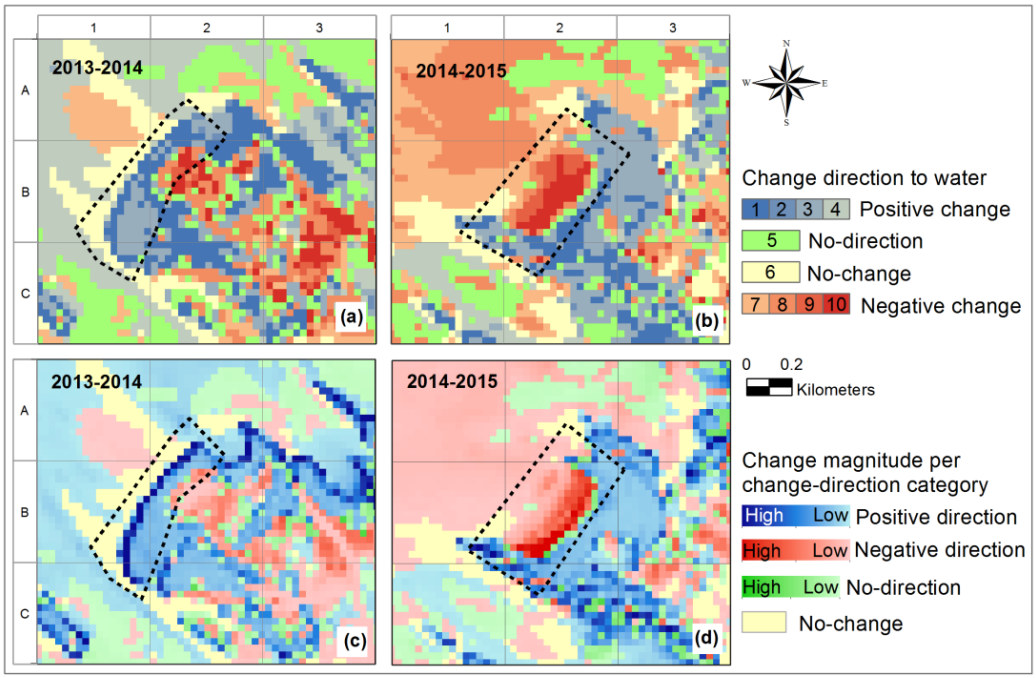

Figure 5. Multi-years pattern of water membership changes showing a high change direction to *positive* (a); and to *negative change* directions (b) with high change magnitude to *positive direction* (c) and to *negative directions* (d).

b) Low change direction and high magnitude; indicates an abrupt change which may result from random events such as coastal flooding triggered by spring tides, extreme waves and winds. Since the magnitude of the changes is high and the change is sudden, this type of change may indicate a higher risk (Figure 6a,d);

c) High direction and low magnitude; indicates a continuous change of an area to be influenced by water which could be be due to cyclical tides and coastal processes, for example changes in the water turbidity (rectangle sites in Figure 6b,e), sediment accretion (ellipse sites in Figure 6b,e), and flooded land. Even though the magnitude is low, since the changes occur frequently, this type of change may also give a higher risk for the area classified as *positive change* direction. In a longer observation, this location may have a risk of coastal inundation as well.

d) Low direction and low magnitude; probably indicate an undisturbed environment. In this study, this category mainly occurs in water areas, probably due to the changes in water turbidity (ellipse sites Figure 6c,f) and in small patches of the coastal land probably resulting from changes in soil moisture (rectangle sites Figure 6c,f).

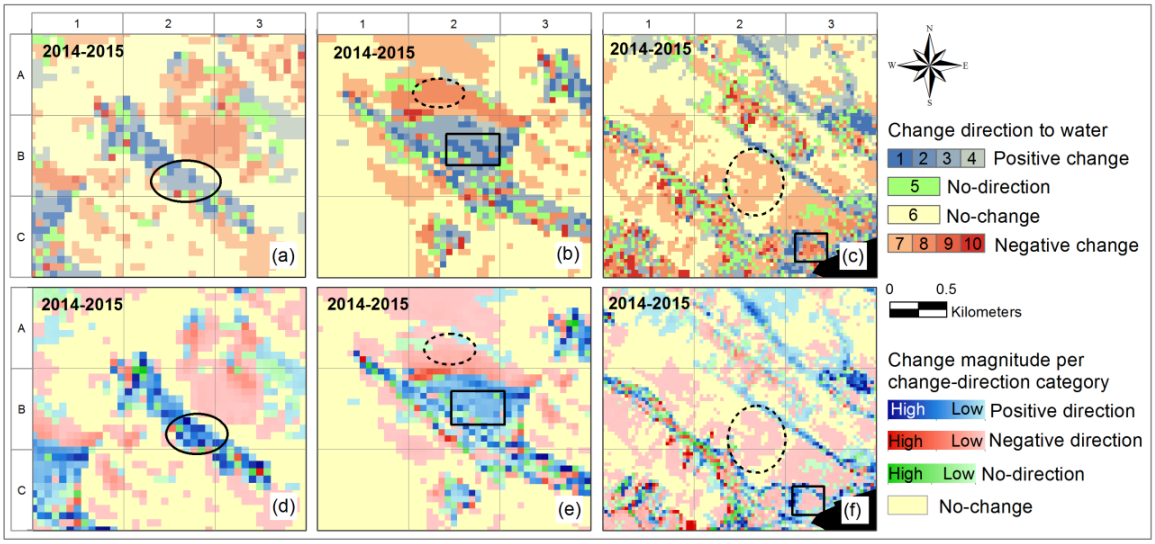

Figure 6. Multi-year patterns of water membership change showing three types of change process occuring in the field: a low change direction to *positive change* (a) with high change magnitude values to *positive direction* (d); a high change direction to *positive change* (b) with low change magnitude values to *positive direction* (e); and a low change direction to *negative change* (c) with low change magnitude values to *positive direction* (f).

4. DISCUSSION

In this study, the dynamics of fuzzy shorelines has been assessed using fuzzy classification and a raster-based change detection technique. FCM classification was used to discriminate the land and water classes and to estimate their memberships. Shorelines and their changes were presented as fuzzy areas and their extents were determined using fuzzy-crisp objects as the *transition zone* between *water* and *non-water*. The change of shoreline was explained in terms of change magnitude and change direction using CVA, allowing us to see the trend of the fluctuating shoreline over time. The uncertainty of the fuzzy shoreline was described by means of confusion indices corresponding to the existential and extential uncertainty of the shoreline. Existential uncertainty expresses the uncertainty of the existence of shoreline in reality. Extensional uncertainty implies that the extent of the shoreline can be determined with limited certainty. In addition, the changed areas of the fuzzy shoreline are thus associated with the distribution of change confusion indices showing the degree of uncertainty of the changes. It can be seen from the results that a location with a higher change magnitude, has higher change confusion as well. This corresponds to the larger differences between the membership and confusion indices in T_1 and T_2. Change direction was assessed to analyse the characteristics of the change by evaluating the membership differences between water memberships for the consecutive years quantifying the overall trend of water membership over the observation period.

The analysis of information provided by the change magnitude and direction using water membership images reveals that each change combination represents a specific type of change process. The processes indicated from the results could vary depending on the locations such as shoreline changes due to floods caused by land subsidence, floods caused by seasonal variation, abrupt shoreline changes due to extreme tides and waves, and the changes of water turbidity and soil moisture triggered by daily weather events. In this research, these specific types of process were explained on the basis of the analysis of four images for each observation period. The seasonal variation of shorelines and whether the changes would lead to a permanent coastal inundation could not be fully assessed because only four observations per year were compared. This shows that the change vector analysis is sensitive to the length of the stacked period.

Analysis of the shoreline changes in the northern coastal area of the Central Java Province shows the changes of shoreline positions from 2013 until 2015. This could be related to the processes that shape shorelines which are determined by the interaction of several factors for example: 1) the change of sea-level; 2) the amount of sediment supplied to the shore by rivers; 3) the movement of the sediment by marine processes; and 4) the role of waves, currents, tides and winds in moving the sediment. Furthermore, sediment transport is not constant, and it is constantly subject to change. The alteration of sediment transport can come from changes in water flow, water level, weather events and human influence. In addition, from the previous studies it has been mentioned that this location has suffered from the changing of shorelines for more than 20 years due to coastal inundation accelerated

by, for example land subsidence, sea-port development, and ground water extraction. Many attempts have been made to combat coastal inundation and erosion of 1.3 kilometres of coast in the study area such as elevated road, raised floor of the house, breakwater, and mangrove planting.

5. Conclusion

In this article, we present a method to identify shoreline positions and their changes as a fuzzy area including a measure of change confusion. Shoreline changes could be detected, and the method provided information regarding the change magnitude and the trend of water membership in every pixel. Our results reveal that this information represents specific type of change processes and shows a multi-year pattern of water membership changes over time. We can conclude that the proposed method can assess changes in a shoreline by taking into account that it is a fuzzy boundary.

The change area estimation, change magnitude and direction of the shorelines may support local government and stakeholders in monitoring the change of fuzzy shorelines. Combining information given by this research with other information such as distribution of population and other facilities could help to determine which location needs to be prioritized in disaster preparedness and response.

6. Reference

Bezdek, J.C., R. Ehrlich, and W. Full. 1984. "FCM: the fuzzy c-means clustering algorithm." *Computers & Geosciences* 10 (2):191-203.

Bird, E.C.F. 1985. *Coastline changes : a global review*: John Wiley and Sons.

Boak, E.H., and I.L. Turner. 2005. "Shoreline definition and detection: a review." *J. Coastal Res* 21 (4):688–703.

Burrough, P.A., P.F.M.V. Gaans, and R. Hootsmans. 1997. "Continuous classification in soil survey: spatial correlation, confusion and boundaries." *Geoderma* 77:115-35.

Cheng, T. 1999. "A process-oriented data model for fuzzy spatial objects." ITC-Wageningen University

Davidson-Arnott, R. 2010. *An introduction to coastal processes and geomorphology*: Cambridge University Press.

Dewi, R.S., W. Bijker, A. Stein, and M.A. Marfai. 2016. "Fuzzy Classification for Shoreline Change Monitoring in a Part of the Northern Coastal Area of Java, Indonesia." *Remote Sensing* 8 (190):1-25.

Ghosh, M.K., L. Kumar, and C. Roy. 2015. "Monitoring the coastline change of Hatiya Island in Bangladesh using remote sensing techniques." *ISPRS J. Photogramm.* 101:137–44.

Hadjimitsis, D.G., G. Papadavid, A. Agapiou, K. Themistocleous, et al. 2010. "Atmospheric correction for satellite remotely sensed data intended for agricultural applications: impact on vegetation indices." *Nat. Hazards Earth. Syst. Sci.* 10:89–95.

Harwitasari, D., and J.A. Van Ast. 2011. "Climate change adaptation in practice: people's responses to tidal flooding in Semarang, Indonesia." *J. Flood Risk Manag.* 4 (3):216-33.

Jin, D., P. Hoagland, D.K. Au, and J. Qiu. 2015. "Shoreline change, seawalls, and coastal property values." *Ocean & Coastal Management - Elsevier* 114: 185-93.

Lambin, E.F., and D. Ehrlich. 1997. "Land-cover Changes in Sub-Saharan Africa (1982-1991): Application of a Change Index Based on Remotely Sensed Surface Temperature and Vegetation Indices at a Continental Scale." *Remote Sensing Environment* 64:181-200.

Lambin, E.F., and A.H. Strahler. 1994. "Change-Vector Analysis in Multitemporal Space: A Tool To Detect and Categorize Land-Cover Change Processes Using High Temporal-Resolution Satellite Data " *REMOTE SENS. ENVIRON.* 48:231-44.

Li, R., R. Ma, and K. Di. 2002. "Digital tide-coordinated shoreline." *Mar. Geod.* 25:27–36.

Lunetta, R.S., and C.D. Elvidge. 1999. *Remote Sensing Change Detection : Environmental Monitoring Methods and Applications*. UK: Taylor & Francis.

Marfai, M.A., H. Almohammad, S. Dey, B. Susanto, et al. 2008. "Coastal dynamic and shoreline mapping: multi-sources spatial data analysis in Semarang Indonesia." *Environ. Monit. Assess.* 142:297–308. doi: 10.1007/s10661-007-9929-2.

Marfai, M.A., and L. King. 2007. "Tidal inundation mapping under enhanced land subsidence in Semarang, Central Java Indonesia." *Nat. Hazards*. doi: 10.1007/s11069-007-9144-z.

Muslim, A.M., G.M. Foody, and P.M. Atkinson. 2006. "Localized soft classification for super-resolution mapping of the shoreline." *Int. J. Remote Sens.* 27 (11):2271–85. doi: 10.1080/01431160500396741.

NWP. 2016. "Water for Food and Ecosystems : Using the Power of Nature." In *Indonesia – The Netherlands Integrated approach of future water challenges*, 26-30. Netherlands: Netherlands Water Partnership (NWP) for the Dutch Government.

O'connor, M.C., J.a.G. Cooper, J. Mckenna, and D.W.T. Jackson. 2010. "Shoreline management in a policy vacuum: A local authority perspective." *Ocean & Coastal Management* 53 (12):769–78.

Pontius, R.G., and M.L. Cheuk. 2006. "A generalized cross-tabulation matrix to compare soft-classified maps at multiple resolutions." *International Journal of Geographical Information Science* 20 (1):1-30.

Senthilnatha, J., V.S. H, S.N. Omkar, and V. Mani. 2012. Spectral-spatial MODIS image analysis using swarm intelligence algorithms and region based segmentation for flood assessment. Paper presented at the Seventh International Conference on Bio-Inspired Computing: Theories and Applications.

Singh, S., and R. Talwar. 2015. "Performance Analysis of Different Threshold Determination Techniques for Change Vector Analysis." *Journal of the Geological Society of India* 86 (1):52-8.

Snoussi, M., T. Ouchani, A. Khouakhi, and I. Niang-Diop. 2009. "Impacts of sea-level rise on the Moroccan coastal zone: Quantifying coastal erosion and flooding in the Tangier Bay." *Geomorphology, Science Direct* 107:32–40.

Tamassoki, E., H. Amiri, and Z. Soleymani. 2014. "Monitoring of shoreline changes using remote sensing (case study: coastal city of Bandar Abbas)." In *7th IGRSM International Remote Sensing & GIS Conference and Exhibition* IOP Publishing.